

## Effect of CeO<sub>2</sub> and CuO oxide nanoparticles on the nickel electroplating in sulfate solution

Mai Van Phuoc<sup>1\*</sup>, Le Thi Phuong Thao<sup>2</sup>

<sup>1</sup>Institute of Materials, Biology and Environment, Academy of Military Science and Technology, 17 Hoang Sam, Nghia Do, Hanoi, Vietnam;

<sup>2</sup>Hanoi University of Mining and Geology, 18 Vien, Dong Ngac, Hanoi, Vietnam.

\*Corresponding author: maivanphuoc\_bk@yahoo.com

Received 7 Sep. 2025; Revised 29 Oct. 2025; Accepted 10 Nov. 2025; Published 28 Nov. 2025.

DOI: <https://doi.org/10.54939/1859-1043.j.mst.107.2025.51-57>

### ABSTRACT

*This study investigates the electrochemical behavior of nickel composite coatings containing CuO and CeO<sub>2</sub> nanoparticles using polarization and electrochemical impedance spectroscopy (EIS). The presence of CuO or CeO<sub>2</sub> oxide nanoparticles in the solution with the ranges between 2 and 12 g/L insignificant increased cathode polarization in the nickel sulfate plating solution. However, the EIS results showed that CuO particles had little effect on the solution resistance and plating process, while CeO<sub>2</sub> particles significantly increased the solution resistance, thus affecting the nickel plating rate. The solution's charge transfer resistance would rise due to the high concentration of added oxide particles, which will be detrimental to the electrode surface's deionization process, the plating solution's oxide particle content should not exceed 12 g/L.*

**Keywords:** Nickel sulfate solution; CeO<sub>2</sub>; CuO; Ni-CeO<sub>2</sub> composite plating; Ni-CuO composite plating.

### 1. INTRODUCTION

Composite coatings are preferable to metallic coatings because they combine the best features of the base metal and the composite material [1]. Nickel-based composite coatings are widely used in a variety of industrial applications due to their distinct mix of exceptional qualities. When compared to pure nickel coatings, these coatings exhibit superior corrosion resistance, wear resistance, and mechanical qualities [1-5]. To create a composite coating, the composite particles are distributed in the plating solution and suspended in the system through agitation. In a composite plating system, the process typically consists of five steps: (1) the formation of ion clouds around the particles, (2) particle convection toward the cathode, (3) particle diffusion through the hydrodynamic boundary layer, (4) particle diffusion through the concentration boundary layer, and (5) particle adsorption on the cathode surface, resulting in deposition on the deposited metal layer [6].

Among the particles, codeposition of nickel, copper oxide (CuO) and cerium oxide (CeO<sub>2</sub>) nanoparticles has attracted attention due to their distinct electrical and chemical properties [2-4]. CuO nanoparticles, being semiconductive, serve as heterogeneous nucleation centers that refine grain structure and enhance the uniformity and conductivity of the deposit [4]. CeO<sub>2</sub> nanoparticles, on the other hand, exhibit strong dielectric properties, forming passive films that significantly improve corrosion resistance [4]. However, their effects on the electrodeposition process differ markedly, particularly in modifying charge transfer, diffusion, and interfacial capacitance.

Electrochemical impedance spectroscopy (EIS) and polarization techniques are powerful methods for exploring such behaviors. EIS provides detailed insights into interfacial resistance, capacitance, and diffusion, while polarization curves identify kinetic changes in metal ion reduction [4, 7, 8]. In this paper, electrochemical impedance and polarization measurements were used to assess the impact of oxide nanoparticles (CuO, CeO<sub>2</sub>) on the plating process in nickel sulfate solution.

### 2. EXPERIMENTAL

#### 2.1. Chemicals

Chemicals used in the study included:  $\text{NiSO}_4 \cdot 7\text{H}_2\text{O}$  (PA, UK),  $\text{H}_3\text{BO}_3$ , sodium lauryl sulfate (PA, China);  $\text{CeO}_2$  particles (Richest Group Ltd., Shanghai, China) and  $\text{CuO}$  particles (Nano Global, Shanghai, China) with sizes of  $50 \div 100$  nm.

## 2.2. Experimental solution

The sulfate plating solution contained  $\text{NiSO}_4 \cdot 7\text{H}_2\text{O}$  (50 - 350 g/L),  $\text{H}_3\text{BO}_3$  (30 g/L), and 0.1 g/L sodium lauryl sulfate ( $S^\circ$  solution). The combined plating solution contained  $S^\circ$  solution ( $\text{NiSO}_4$  300 g/L) and  $x$  g/L  $\text{CuO}$  ( $x = 2 \div 14$ ; symbol  $S^\circ\text{Cu}^x$ ) or  $y$  g/L  $\text{CeO}_2$  ( $y = 2 \div 14$ ; symbol  $S^\circ\text{Ce}^y$ ). The nanoparticles were wetted with sodium lauryl sulfate before being evenly dispersed in the solution by ultrasound. The plating solution was stirred continuously to maintain the dispersion of the nanoparticles.

## 2.3. Methods

The cathodic polarization curve of the Ni plating process was measured using an Autolab PG302 device (Netherlands) with a three-electrode system: a fixed nickel electrode with an area of  $1 \text{ cm}^2$  served as the working electrode, a Ti plate measuring with an area of  $10 \text{ cm}^2$  served as the counter electrode, and a silver-silver chloride electrode saturated  $\text{Ag}/\text{AgCl}$  as the reference electrode. The potential scanning area was from open circuit potential (OCP) to  $-2.0 \text{ V}$ , the scanning speed was  $10 \text{ mV/s}$ , and the solution temperature was  $50^\circ\text{C}$ .

The impedance of the Ni plating process was measured using an IM6 device (Zahner-Elektrik, Germany) with a three-electrode system: a fixed nickel electrode with an area of  $0.5 \text{ cm}^2$  served as the working electrode, a Ti plate with an area of  $10 \text{ cm}^2$  served as the counter electrode, and a calomel electrode served as the reference electrode. The survey range was between  $100 \text{ kHz}$  and  $10 \text{ mHz}$ , and the solution temperature was set at  $50^\circ\text{C}$ .

## 3. RESULTS AND DISCUSSION

### 3.1. Cathodic polarization curves of the Ni in the plating solutions

#### 3.1.1. Cathodic polarization curves of the Ni in the nickel sulfate solution

To investigate the influence of  $\text{NiSO}_4$  concentration on plating layer quality and plating conditions, polarization potential was evaluated in solutions containing various  $\text{NiSO}_4$  concentrations. The results are displayed in figure 1.

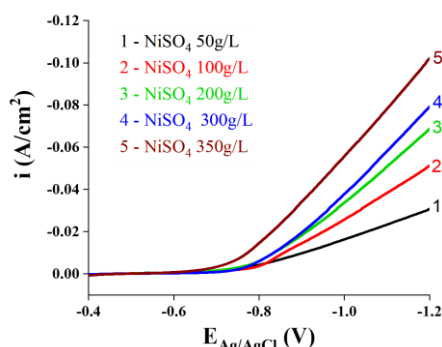


**Figure 1.** Cathodic polarization curves of Ni in the nickel sulfate solutions ( $S^\circ$ ) with difference  $\text{NiSO}_4$  concentrations ( $50 \div 350$  g/L).

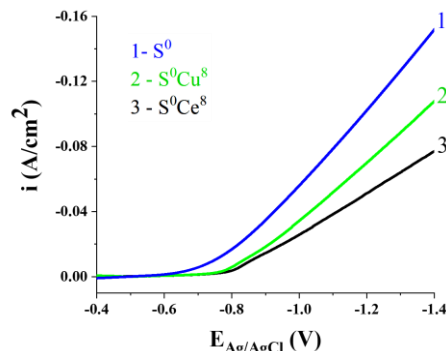


**Figure 2.** Cathodic polarization curves of Ni in the  $S^\circ$ ,  $S^\circ\text{Cu}^8$ ,  $S^\circ\text{Ce}^8$  solutions.

Figure 1 showed that the discharge potential of  $\text{Ni}^{2+}$  in the tested solution was around  $-0.67\text{V}$  ( $\text{Ag}/\text{AgCl}$ ) (line 1), which was more negative than the discharge potential of hydrogen, indicating that  $\text{H}_2$  gas was always released during the nickel plating process [8]. In the nickel sulfate plating solution,  $\text{H}^+$  ions were reduced first, followed by  $\text{Ni}^{2+}$  ions to produce the Ni plating layer; the  $\text{Ni}^{2+}$  ion reduction process resulted in the creation of the intermediate ion  $\text{Ni}(\text{OH})^+$  [8, 9]. The plating

process in nickel sulfate solution can be described according to reactions (1) – (7), in which reactions (1) – (3) occurred simultaneously in the same potential region as reactions (4) – (7) [9]:



The findings (figure 1) reveal that when the concentration of NiSO<sub>4</sub> in the solution increased, the polarity decreased because the amount of Ni<sup>2+</sup> ions in the solution increased, the plating speed increased. However, too high amount of NiSO<sub>4</sub> will be difficult to dissolve during the composting process. Therefore, the concentration of NiSO<sub>4</sub> was set to 300 g/L.

### 3.1.2. Effect of CeO<sub>2</sub> and CuO oxide particles on polarization curves in nickel sulfate plating solution

The nickel polarization curves in figure 2 demonstrated that Ni's discharge potential in sulfate solution was E\* = -0.70 V (Ag/AgCl). When CeO<sub>2</sub> or CuO oxide particles were added to the solution (both at 8 g/L), the cathode polarization increased relative to the initial nickel sulfate plating solution, but the shape of the polarization curve remained unchanged. This is because when CeO<sub>2</sub>/CuO oxide nano particles are present in the plating solution, Ni<sup>2+</sup> ions are adsorbed onto their surfaces, bringing them to the cathode area to co-precipitate with Ni to form a composite plating layer. As a result, the concentration of free Ni<sup>2+</sup> ions in the plating solution decreases, resulting in a decrease in plating speed or an increase in cathode polarization. This phenomenon is similar to other Ni composite plating layer creation processes [8].

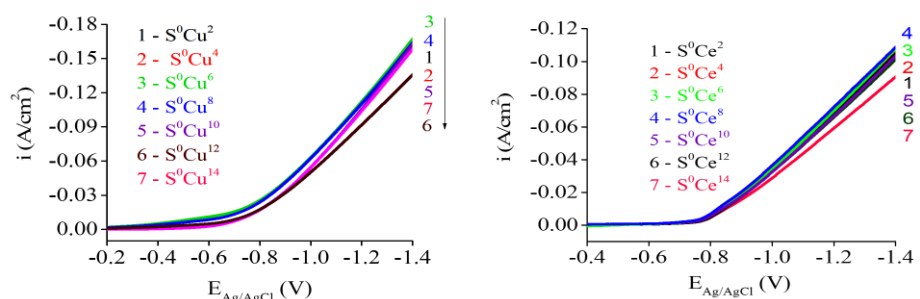


Figure 3. Cathodic polarization curves of Ni in solutions of S<sup>0</sup>Cu<sup>x</sup> (x = 2 ÷ 14 g/L) and S<sup>0</sup>Ce<sup>y</sup> (y = 2 ÷ 14 g/L).

Particle concentration and type often have a significant impact on the plating process and the characteristics of the composite plating layer that is created [6]. When the concentration of each oxide in the solution was increased from 2 to 12 g/L, the cathodic polarization of nickel remained nearly constant (figure 2). When the concentration of particles in the solution reached 14 g/L, cathodic polarization increased. The polarization curve graph shows the discharge of Ni<sup>2+</sup> ions at the potential E\* = - 0.66 V (Ag/AgCl) in the composite plating solution (S<sup>0</sup>Ce<sup>y</sup> or S<sup>0</sup>Cu<sup>x</sup>) as particle concentration changed from 2 to 14 g/L (figure 3).

## 3.2. In-situ electrochemical impedance spectra (EIS) of the studied electrode in the sulfate plating solution

### 3.2.1. EIS of the studied electrode in the sulfate plating solution

According to figure 1's polarization curve measurement data, the Ni discharge process in the

sulfate solution started at potential  $E^* = -0.70$  V (Ag/AgCl), or  $-0.744$  V (with respect to the Calomen electrode-SCE), and was steady at a potential of  $-0.834$  V (SCE).

Figure 4 depicts the Nyquist impedance spectra of the investigated electrode measured at various potential regions in the nickel sulfate plating solution  $S^0$  ( $\text{NiSO}_4$  300 g/L,  $\text{H}_3\text{BO}_3$  30 g/L, sodium lauryl sulfate 0.1 g/L). The symbols represented the actual measured values, whereas the solid lines corresponded to the simulation lines. The results demonstrated that the simulation lines were nearly equal to the measured values. The simulation data are shown in table 1.

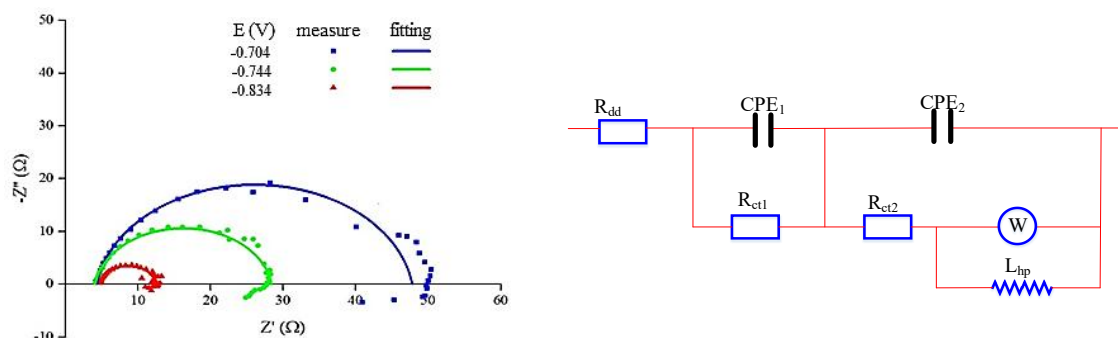


**Figure 4.** Nyquist impedance spectra of the studied electrode in  $S^0$  solution at different potentials and the equivalent diagram.

The equivalent circuit design (figure 4) was made up of two consecutive semicircles: the first semicircle contained the constant phase component ( $\text{CPE}_1$ ) and the charge transfer resistor ( $R_{ct1}$ ), and the second semicircle had the remaining four components ( $\text{CPE}_2$ ,  $R_{ct2}$ ,  $W$ ,  $L_{hp}$ ). Thus, the diffusion and adsorption of  $\text{NiOH}^+$  ions (an intermediate product in the nickel plating process in nickel sulfate solution [9]) onto the electrode surface occurred simultaneously. However, in figure 4, it was difficult to distinguish these two semicircles because the existence of  $\text{CPE}_1$  and  $\text{CPE}_2$  flattened the two semicircles; Thus, when joined in series, they appeared to be one semicircle.

**Table 1.** Values of components in the equivalent diagram of the studied electrode in the  $S^0$  solution system at different potentials.

E (V)	$R_{dd}$ ( $\Omega$ )	$\text{CPE}_1$		$R_{ct1}$ ( $\Omega$ )	$\text{CPE}_2$		$R_{ct2}$ (m $\Omega$ )	$\sigma$ (m $\Omega \cdot \text{s}^{-1/2}$ )	$L_{hp}$ (H)
		( $\mu\text{F}$ )	m		(F)	m			
-0.704	4.323	28.07	0.909	43.47	6.099	0.612	88.53	195.3	22.25
-0.744	4.127	28.31	0.913	24.27	13.75	0.491	42.56	119.4	37.14
-0.834	4.396	25.40	0.919	7.823	61.57	0.333	18.14	52.08	42.70

The findings in table 1 demonstrated that when the sweep potential moved in a more negative direction, the values of Warburg impedance and charge transfer resistance both dramatically dropped. The reason was that just a double layer was generated at the potential of  $-0.704$  V since the  $\text{Ni}^{2+}$  discharge process had hardly begun. At a potential of  $-0.744$  V, these resistance values had dropped as the Ni discharge process had commenced. The reduction of  $\text{Ni-H}_{ads}$  on the electrode surface caused a larger release of  $\text{H}_2$  gas, particularly at  $-0.834$  V, as did the reduction of  $\text{NiOH}^+$  ions. Thus, the process of plating Ni from the  $S^0$  sulfate solution system involved two processes: diffusion and adsorption on the electrode surface.

The diffusion coefficient was calculated by the following equation [10]:

$$D = \frac{2R^2T^2}{n^4F^4A^2C^2\sigma^2}$$

In which:  $\sigma$  was Warburg constant ( $\Omega \text{ s}^{-1/2}$ );  $A$  was electrode surface area ( $0.5 \text{ cm}^2$ );  $n$  was the

number of electrons exchanged ( $n = 2$ );  $T$  was the absolute temperature of the plating solution (323 K);  $R$  was Boltzman gas constant (8.314 J/mol.K);  $F$  was Faraday constant (96500 C/mol);  $C$  was the concentration of oxidizing/reducing agent on the electrode ( $C = 1 \text{ mol/cm}^3$ ). The values of  $D$  during the nickel plating process at potential values of -0.704 V, -0.744 V, and -0.834 V (SCE) were  $1.09\text{E-}12$ ,  $2.92\text{E-}12$ ,  $1.54\text{E-}11 \text{ (cm}^2/\text{s)}$ , respectively. These results demonstrated that the more negative the discharge potential is, the larger the diffusion coefficient is, meaning that the diffusion of ions occurred more easily, so the reaction rate is faster. This is consistent with the results of measuring the cathodic polarization curve of the  $\text{S}^0$  solution (figure 1).

3.2.2. Effect of oxide nanoparticles on electrochemical impedance spectrum in nickel sulfate plating solution

The impedance spectrum of the  $\text{S}^0\text{Cu}^x$ ,  $\text{S}^0\text{Ce}^y$  solution system was used to assess the impact of oxide nanoparticles ( $\text{CuO}$ ,  $\text{CeO}_2$ ) on the nickel plating process in the sulfate combination plating solution. Based on the findings of the impedance spectrum assessment in the  $\text{S}^0$  plating solution previously examined, the potential  $E = -0.834 \text{ V}$  was chosen to measure the impedance spectrum.

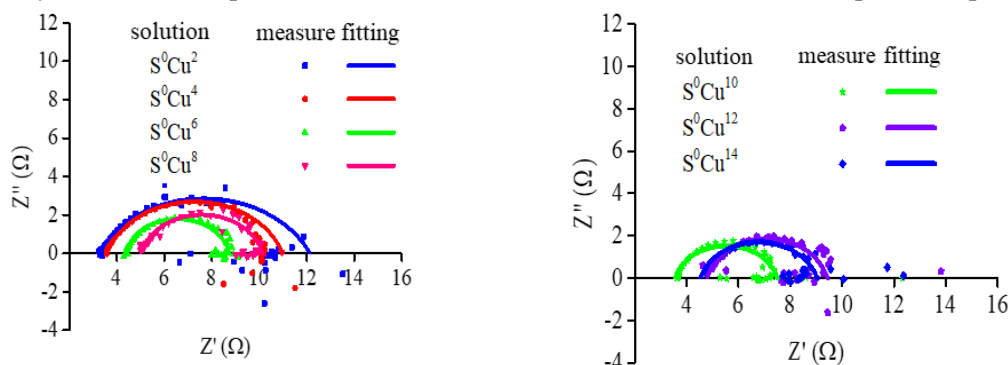


Figure 5. Nyquist impedance spectra of the studied electrode in  $\text{S}^0\text{Cu}^x$  solution ( $x = 2 \div 14 \text{ g/L}$ ) at -0.834 V.

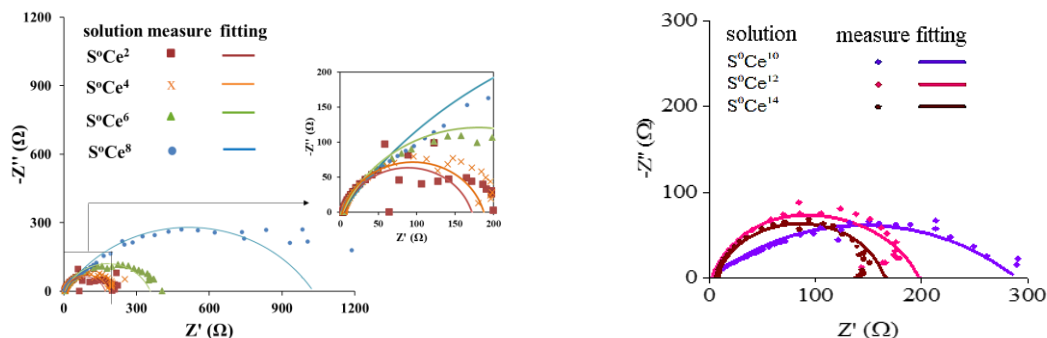


Figure 6. Nyquist impedance spectra of the studied electrode in  $\text{S}^0\text{Ce}^y$  solution ( $y = 2 \div 14 \text{ g/L}$ ) at -0.834 V.

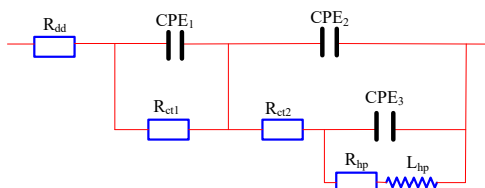


Figure 7. Equivalent diagram of Nyquist spectra in nickel sulfate solution consisting of  $\text{CuO/CeO}_2$ .

The results (figure 5, figure 6) showed that the simulation and experimental lines were very similar, so the equivalent circuit in figure 7 was consistent with the nickel discharge process in a nickel sulfate plating solution with added CuO or CeO<sub>2</sub> nano composite particles. The equivalent circuit model in figure comprised R<sub>s</sub>, two constant phase elements (CPE<sub>1</sub> and CPE<sub>2</sub>), and two charge-transfer resistances (R<sub>ct1</sub> and R<sub>ct2</sub>) in parallel branches - indicating that the system's electrochemical response included both double-layer charging and faradaic processes. CPE<sub>1</sub> was associated with the capacitive behavior of the electrical double layer, while CPE<sub>2</sub> and CPE<sub>3</sub> represent non-ideal interfacial capacitance arising from surface roughness and nanoparticle incorporation. The presence of the inductive branch (L<sub>hp</sub>) reflected the possible adsorption/desorption phenomena during metal nucleation.

When CuO nanoparticles were introduced in the solution, R<sub>ct1</sub> increased slightly from 3.9 Ω (S°Cu<sup>2</sup>) to 8.5 Ω (S°Cu<sup>14</sup>), suggesting a moderate retardation of electron transfer, yet CuO particles may improve surface uniformity and deposition stability [5]. Conversely, CeO<sub>2</sub>-containing baths exhibited significantly larger semicircles, with R<sub>ct1</sub> ranging from 124 Ω (S°Ce<sup>2</sup>) to 354 Ω (S°Ce<sup>14</sup>), indicating strong inhibition of charge transfer, as CeO<sub>2</sub> particles act as dielectric barriers that restrict Ni<sup>2+</sup> reduction and promote formation of compact, passivating films [2, 3]. This result was consistent with the polarization measurements (figure 2), where the cathode polarization increased more when the solution had CeO<sub>2</sub> particles than in the case of CuO.

#### 4. CONCLUSIONS

The presence of CuO or CeO<sub>2</sub> oxide nanoparticles in the solution increased cathode polarization in the nickel sulfate plating solution; however, the change was insignificant when the particle content in the plating solution ranged between 2 and 12 g/L, and the shape of the cathode polarization curve remained constant. The EIS results demonstrate that the Ni plating process consisted of diffusion and adsorption processes; When CuO or CeO<sub>2</sub> particles were added to the plating solution, an inductive component appeared with the adsorption process. The incorporation of CeO<sub>2</sub> nanoparticles alters solution conductivity and charge transfer kinetics more significantly than CuO, indicating stronger particle-ion interaction during Ni co-deposition. The impact of CuO and CeO<sub>2</sub> nanoparticles on the nickel layer will be evaluated more clearly in subsequent studies on the morphology, microstructure, corrosion behavior of the coatings.

#### REFERENCES

- [1]. D. M. Zellele, G. S. Yar-Mukhamedova, and M. Rutkowska-Gorczyca, "A Review on Properties of Electrodeposited Nickel Composite Coatings: Ni-Al<sub>2</sub>O<sub>3</sub>, Ni-SiC, Ni-ZrO<sub>2</sub>, Ni-TiO<sub>2</sub> and Ni-WC," Materials (Basel), Vol. 17, No. 23, (2024).
- [2]. I. Makarava et al., "Influence of CeO<sub>2</sub> and TiO<sub>2</sub> Particles on Physicochemical Properties of Composite Nickel Coatings Electrodeposited at Ambient Temperature," Materials (Basel), Vol. 15, No. 16, (2022).
- [3]. W. Zhang, Z. Yuan, A. Sun, J. Liu, and M. Xiao, "Preparation and investigation of Ni-W/CeO<sub>2</sub> composite coating and its structure and anti-corrosion properties with different ceria content and deposition time," Ceramics International, Vol. 50, No. 21, pp. 44560-44571, (2024).
- [4]. H. Rao, W. Li, Z. Luo, H. Liu, L. Zhu, and H. Chen, "Nucleation and growth mechanism of Ni/SiC composite coatings electrodeposited with micro- and nano-SiC particles," Journal of Materials Research and Technology, Vol. 30, pp. 3079-3091, (2024).
- [5]. M. Wang et al., "Influence of CuO addition on the microstructure, exothermic characteristics and mechanical properties of Al/Ni/CuO energetic structural materials prepared by friction stir additive manufacturing," Journal of Materials Research and Technology, Vol. 35, pp. 6537-6550, (2025).
- [6]. T. Guan and N. Zhang, "Recent Advances in Electrodeposition of Nickel-Based Nanocomposites Enhanced with Lubricating Nanoparticles," Nanomanuf Metrol, Vol. 7, No. 1, p. 25, (2024).
- [7]. R. Wiart, "Elementary steps of electrodeposition analysed by means of impedance spectroscopy," Electrochimica Acta, Vol. 35, No. 10, pp. 1587-1593, (1990).
- [8]. Y. Abdesselam, A. Belloufi, I. Rezugui, M. Abdelkrim, T. Catalin, and B. Chiriță, "Composite coatings

- based on nickel and  $Y_2O_3$  nanoparticles: a comprehensive analysis of developments in electrodeposition and functional property optimization," *The International Journal of Advanced Manufacturing Technology*, Vol. 137, No. 7-8, pp. 3273-3332, (2025).
- [9]. R. Oriňáková, M. Strečková, L. Trnková, R. Rozik, and M. Gálová, "Comparison of chloride and sulphate electrolytes in nickel electrodeposition on a paraffin impregnated graphite electrode," *Journal of Electroanalytical Chemistry*, Vol. 594, No. 2, pp. 152-159, (2006).
- [10]. Zahner Meßsystem, "Thales Softwave Package for Electrochemical Workstations User Manual," Germany, (2007).

### TÓM TẮT

#### **Đặc điểm quá trình mạ trong dung dịch niken sunphat khi có mặt các hạt nano oxit $CeO_2$ , $CuO$**

Nghiên cứu này khảo sát tính chất điện hóa của quá trình tạo lớp mạ niken trong dung dịch niken sunphat với các hạt nano oxit  $CuO$  và  $CeO_2$  thông qua phương pháp đo đường cong phân cực và phổ tổng trở (EIS). Với hàm lượng các hạt  $CuO$  hoặc  $CeO_2$  trong dung dịch trong khoảng 2 đến 12 g/L, độ phân cực catốt của niken tăng không đáng kể. Tuy nhiên kết quả EIS cho thấy, các hạt  $CuO$  ít ảnh hưởng đến điện trở dung dịch và quá trình mạ nhưng các hạt  $CeO_2$  lại làm tăng đáng kể điện trở dung dịch, do đó ảnh hưởng đến tốc độ mạ niken. Do điện trở chuyển điện tích của dung dịch sẽ tăng khi nồng độ của các hạt oxit trong dung dịch mạ tăng, điều này sẽ gây bất lợi cho quá trình khử ion của bề mặt điện cực, nên hàm lượng hạt oxit trong dung dịch mạ không nên vượt quá 12 g/L.

**Từ khoá:** Niken sunphat;  $CeO_2$ ;  $CuO$ ; Lớp mạ Ni- $CeO_2$ ; Lớp mạ Ni- $CuO$ .